AERODYNAMIC INTERACTIONS FOR A FAN-IN-WING CONFIGURATION IN HOVER

Naipei P. Bi David J. Haas Anish J. Sydney Kevin R. Kimmel

Naval Surface Warfare Center Carderock Division
West Bethesda, MD, USA

ABSTRACT

A series of hover tests have been conducted for an isolated fan model and a generic fan-in-wing model in the 8- by 10-ft Subsonic Wind Tunnel at the Naval Surface Warfare Center Carderock Division, USA. The objectives of these wind tunnel tests are to establish a benchmark data set that can be used to verify and validate Computational Fluid Dynamics and other predictive methods. This data set can also be used to better understand the mutual aerodynamic interactions between a fan and its surrounding wing. To make the data set representative and comprehensive, while the wing geometry was kept unchanged during tests, several key fan design parameters were varied, which included fan solidity, number of blades, blade twist distribution as well as the fan rpm and collective pitch. Fan axial location within the duct was also varied. In this investigation, specific effort was made to identify and separate out the individual contributions of the fan and the wing to the overall fan-in-wing model aerodynamic performance. To accomplish this, a uniquely designed fan balance along with a cantilevered fan support system and an innovative safety device called the motion limiting mechanism were utilized during the tests. The setup allowed the fan thrust to be measured by the fan balance independently while the overall aerodynamic forces and moments of the complete fan-in-wing model were measured by a wind tunnel six-component balance. In addition, 169 pressure taps were distributed at critical locations over the wing surface, near and around the duct inlet as well as on the duct walls inside the duct. The independent fan thrust and large number of pressures measured provide much needed insight into the interactional aerodynamic phenomenon between the fan and wing. A large volume of data were obtained and a systematic analysis of the data is underway. The results to be presented in this paper include the initial analysis of pressures measured near and around the duct inlet, the fan aerodynamic performance with and without the surrounding wing, and the overall aerodynamic performance of the fan-in-wing model. The results have shown that the aerodynamic interactions between the fan and wing are mutually beneficial and the fan aerodynamic characteristics are altered significantly due to the presence of the wing, which indicates strongly that an integrated design philosophy should be utilized for fan-in-wing system to optimize its overall aerodynamic performance.

NOMENCLATURE

R	blade radius
c	blade chord
e	root cutout
A	fan disk area, = πR^2
N_b	number of blades
ρ	air density
Ω	fan rotational frequency
P	fan power, hp
T	total (fan-in-wing) thrust, lbs
T_R	fan thrust, lbs
C_{TR}	fan thrust coefficient, = $T_R/(\rho A\Omega^2 R^2)$
C_T	total (FIW) thrust coefficient, = $T/(\rho A\Omega^2 R^2)$
C_P	power coefficient, = $P/(\rho A\Omega^3 R^3)$
σ	fan solidity ratio, = $N_b\, c(R-e)/A$
C_T/σ	total blade loading coefficient
C_{TR}/σ	fan blade loading coefficient
C_P/σ	power loading coefficient
DL	disk loading, =T/A, psf
P	wing pressure, psf
PL	power loading, =T/P, lb/hp

INTRODUCTION

Recently, a program called the Vertical Take-Off and Landing (VTOL) X-plane technology demonstrator was launched by DARPA, which aims to develop an aircraft that push the boundaries of both VTOL efficiency and cruise efficiency at a high forward flight speed (300–400 knots) [1]. Various configurations have been proposed to meet these challenging goals and several use Lift Fan and/or Fan-in-Wing (FIW) technologies. For example, one configuration proposed by Boeing called Phantom Swift, uses two body fans that are mainly for VTOL operations and two tilting ducted fans that are for both VTOL and forward flight [2]. Another configuration proposed by Aurora is called Lightning Strike, which uses a total of 24 ducted fans uniquely distributed along the wings to perform both VTOL and high speed forward flight [3]. One of the reasons various lift fan technologies are proposed for future VTOL aircraft is that any vehicle with lift fan technology

Presented at the European Rotorcraft Forum 42, Lille, France, September 6 – 8, 2016.

that includes a ducted fan, body fan, or FIW can have the potential of combining the aerodynamic advantages of both rotary and fixed wing aircraft. While there are some distinguishing aerodynamic characteristics between various lift fan configurations (ducted fan, body fan, FIW, etc.), it is understood that compared to an equal size open fan, an embedded lift fan configuration provides aerodynamic benefits in terms of enhancing the thrust capability and improving the efficiency in hover.

In fact, over the past several decades there has been continuing interest in how to take advantage of both rotorcraft and fixed wing aircraft aerodynamics to develop an air vehicle that can fly at high speed (like fixed wing aircraft) and possess sustained hover capability (like conventional rotorcraft). Fan-in-wing configurations have been considered particularly promising. For example, the GE-Ryan XV-5 aircraft was developed and manufactured in the 1960s and 1970s [4] with the support of several US government agencies including NASA, the Army, and the Navy. The XV-5 aircraft was equipped with three fans, two of which were embedded inside the wing and the third embedded inside the nose of the fuselage. The XV-5 had VTOL capability and was tested up to a speed of exceeding 400 knots. In the early 2000's, Northrop Grumman developed an Unmanned Air-cargo System concept called Maritime Unmanned Vertical Replenishment (MUVR) using a similar FIW system of that employed by the Ryan XV-5 aircraft. This vehicle was designed for ship-to-shore resupply and can fly at a speed exceeding 200 knots [5]. Another recent concept that uses FIW technology is the VTOL Advanced Reconnaissance Insertion Organic Unmanned System **(**VARIOUS**)** developed by Lockheed Martin, which is an Unmanned Air System (UAV) and is designed to support special forces and expeditionary units of marines [6]. Outside of the US, among others, Urban Aeronautics in Israel is now developing an aircraft called X-hawk that uses two embedded fans in a blended body [7].

While FIW technology has advantages, it has a few technical challenges that need to be understood and overcome in order to fully exploit its benefits. One of the challenges is that hover efficiency is much lower than conventional rotorcraft due mainly to (1) very high values of fan disk loading used and (2) the lack of progress in new fan development because of limited understanding of fan performance when the fan is embedded within a wing. Therefore, to improve hover efficiency, it is necessary to rethink the practical range of disk loading to be used and to have a full understanding of the mutual aerodynamic interactions between the fan and wing. Another technical challenge during the FIW aircraft development in the past was its poor controllability due mainly to the adverse aerodynamics such as the large momentum drag and the nose-up pitching moments in transition (from hover to high speed forward flight). The use of auxiliary lifting devices such as a fan embedded into the fuselage nose, or a jet in the rear fuselage, and/or duct exit vanes may improve controllability for specific FIW designs. However, to use any of these methods efficiently requires comprehensive understanding of the underlying source of these challenges.

Currently, there is a dearth of data that can provide insight into the mutual aerodynamic interactions between a fan and wing, which includes the full knowledge of individual contribution from the fan and from the wing to the overall thrust as well as the detailed pressure distribution at critical locations over the wing and duct surfaces. There are generally two approaches to obtain the detailed aerodynamic information needed: CFD and wind tunnel test. However, The CFD approach has not been comprehensively validated for the FIW configuration by benchmark test data, which leads back to the second approach – to use the wind tunnel test to obtain the detailed aerodynamic information for FIW configuration.

In the current study, a series of hover tests have been conducted for an isolated fan model and a generic fan-in-wing model. These tests have generated a large volume of test data and systematic analysis of the test data is underway. Some initial results on the basic aerodynamic performance have been published in Ref. [8-9]. This paper specifically concentrates on the initial analysis of the mutual aerodynamic interactions between the fan and wing including pressures measured near and around the duct inlet as well as fan aerodynamic performance with and without a surrounding wing.

DESCRIPTION OF EXPERIMENTS

Test Facility

All of the experiments were performed in the Naval Surface Warfare Center Carderock Division 8- by 10-ft closed-circuit Subsonic Wind Tunnel (SWT). The tunnel wind speed range is from 10 to 275 ft/sec (6 to 163 kt) and the test section static pressure is atmospheric. It is a fact that conducting any fan or lift fan hover test in a closed circuit facility can generate undesirable air flow recirculation inside the tunnel when the fan rotational axis is parallel to the tunnel airflow direction. This recirculating flow results directly from the fan downwash, which forces the fan to be operating in an "ascending" condition in hover. Other researchers found that the tunnel recirculation flow speed could be as high as 20 knots for a conventional ducted fan test, which severely distorted the hover test

results and is hard to be corrected accurately. However, the flow recirculation due to the fan downwash in hover can be prevented in the NSWCCD SWT because this tunnel is equipped with three access doors along the tunnel flow circuit. To block the flow recirculation during tests, a polyethylene tarp was placed on the screens of one of the corner guide vanes of the tunnel to block the flow path completely and all three access doors were open during the tests such that air could enter the tunnel from one door and exit from the other two doors. A schematic of the facility flow circuit with the tarp, photographs of access doors and power section are shown in Fig. 1. Also, during the tests, a pitot static probe was used to closely monitor the magnitude of any possible reverse flow downstream of the model and only benign reverse flow velocities were found.

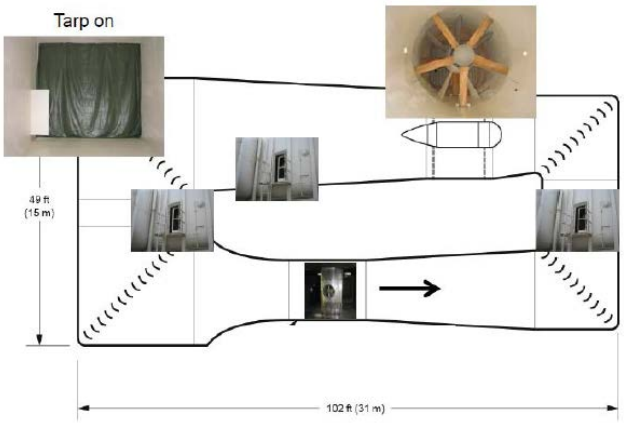

Figure 1: A schematic of the facility flow circuit with the tarp on and access doors open

Model

The FIW model consists of a generic wing and a fan configuration suitable for parametric studies. The wing size is 48" by 48" with an airfoil of NACA 65-218, which provides a reasonable wing thickness to house a single fan or a co-axial fan configuration. The duct consists of three parts: an inlet, a wall, and an exit ring, all of which are made of Stereolithography (SLA) and can be reconfigurable such that the duct inlet radius and the duct wall divergence angle can be varied as required. The duct diameter is 24", centered along the wing spanwise direction. The duct location along the wing chordwise direction is optimized such that the duct depths at the forward and the aft end of the duct on the centerline of wing are equal. The model was mounted vertically in the wind tunnel on a rotating strut that was supported by an external six-component balance [9]. There are fairings with the same airfoil shape as the wing above and below the wing extending the wing outer mold line to the wind tunnel floor and ceiling, as shown in Fig. 2. The fairings are supported by the floor and ceiling and are

a. Complete FIW

b. Isolated fan

Figure 2: Models installed in test section of NSWCCD wind tunnel

physically separated from the wing. The fairings provide an aerodynamic extension from the wing to the wind tunnel floor and ceiling and shield the balance strut extension hardware and the mid-wing spar from air loads due to the wind in the tunnel. A small gap must be maintained between the wing model and the fairings to prevent fouling of the balance force and moment measurements. A series of fouling circuits were installed to detect contact between the model and sections of fairing. Figure 2a and 2b show the complete FIW model and the isolated fan model installed in the test section of wind tunnel respectively.

Figure 3 shows a diagram of the fan/hub system, which consists of the hub, spindle, and blades. Each blade is attached to the blade spindle with six bolts and two washers that distribute the loads over the entire blade flange. For clarity, the details of bolts and washers are not shown in Fig. 3. The spindle is bolted

to the fan hub. The hub bolt pattern allows the blade

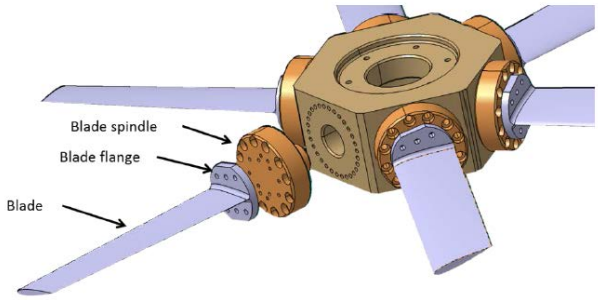

Figure 3: Diagram of fan hub system

spindle pitch to be incremented in eight-degree increments. There are two bolt patterns in the blade spindle that allow the blade to be positioned in four-degree increments. There are two sets of blade spindles that differ by a two-degree increment, allowing the blade collective pitch to be set with a resolution of 2 degrees from 0 to 360 degrees. Three sets of six blades are used in the experiments; -12° twist, +12° twist, and -12° twist with double the normal chord and thickness. Only results for the first set of blades are discussed in this paper. The clearance between the blade tip and duct wall is approximately 0.125".

Figure 4 shows the schematic of the fan drivetrain used in the test, which includes high-speed bearings, two Lovejoy flexible couplings, a torque gage to measure the power consumed by the fan, and a water-cooled, electrically driven motor. The entire drivetrain is mounted on a cantilevered strut. The novel cantilever design is what allows the loads from the fan and the wing to be measured independently [9]. The drivetrain is mounted on top of the thrust gage, which is oriented such that it can solely measure the thrust of the fan, as shown by Fig. 4. Because the fan is decoupled structurally from the wing, the fan thrust balance measures only the axial thrust from the fan. The thrust gage and drivetrain assembly are mounted to a dovetail mechanism that allows the axial fan position to be varied within the duct. This mechanism was then mounted to a curved strut that is cantilevered off of the main wing strut. The wing strut is, in turn, mounted to the wind tunnel six-component balance which measures all six components of forces and moments on the entire FIW model.

It should be emphasized that the decision of using a cantilevered design without stators connecting to the wing makes minimizing drivetrain system vibrations particularly important in order to prevent the potential striking of the fan blades with the duct wall. To the author's knowledge, this design is unprecedented. In the model design, assembly and test preparation, a rather tedious and sophisticated procedure was used to align all components of the drivetrain in the lab as much as possible prior to the installation in the wind tunnel. Also, to have an additional safety feature, an innovative safety device called the Motion Limiting Mechanism (MLM) was designed and used. This device limits the maximum fan in-plane motion to be smaller than the clearance between the blade tip and duct wall, but allows the fan to have an out of plane motion freely so as not to affect the fan thrust

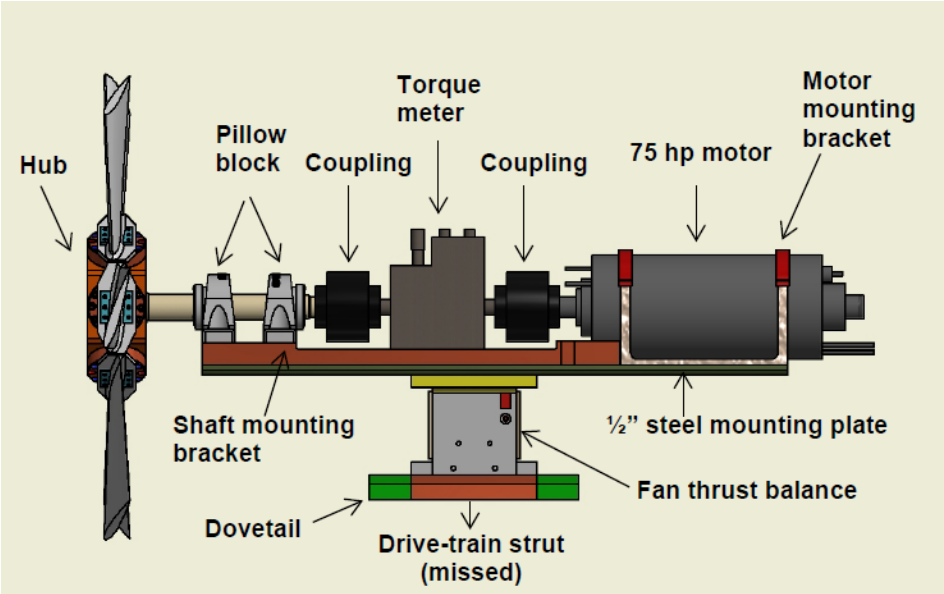

Figure 4: Schematic of fan drivetrain

measurements.

The model has five groups of pressure taps (a total of 169 individual taps) to measure the pressures in the following areas: near and around the duct inlet around the duct circumferential azimuth (azimuth zero at the leading edge of duct and 90^{o} is on the advancing side), on the upstream duct wall panel, on the downstream duct wall panel, on the upper skin of wing, and on the lower skin of wing. In this paper, focus is placed on the initial analysis of the first group of pressures, i.e., pressures around the duct inlets at every 30^{o} of azimuth angle around the duct circumference. There are 5 pressure taps around the duct inlet at each section, two on the straight portion of the wing skin near the duct inlet and three on the curved portion around the duct inlet lip. Figure 5 shows a schematic of pressures taps and indexes around the duct inlets at azimuth = 0, 90, 180, and 270 deg.

Test Variables and Procedure

For both isolated fan and FIW configurations, wind tunnel tests were conducted over a range of operating conditions including fan rotational frequency (rpm), fan blade collective pitch, fan solidity, number of blades, and blade twist. For the FIW configuration, two different fan axial positions within the duct were tested. Depending on the configuration, the blade collective pitch was varied from -6° to +54° to ensure that a wide range of aerodynamic characteristics including the post stall characteristics were captured. The fan rotational frequency was varied but limited to a maximum of 4,250 rpm after initial runs showed that higher fan rpm had benign effects on non-dimensional aerodynamic characteristics. The fan rotational speed was incrementally raised to the highest rpm, with data being collected at each increment. Data were also collected at selected rotational frequencies as the fan was spun back down to determine if there were any hysteresis effects in the data.

In addition, data were collected at 0 rpm at both ends of the rpm sweep and then used as a tare if needed. Once data for an entire configuration were acquired, a new configuration was set-up and the process

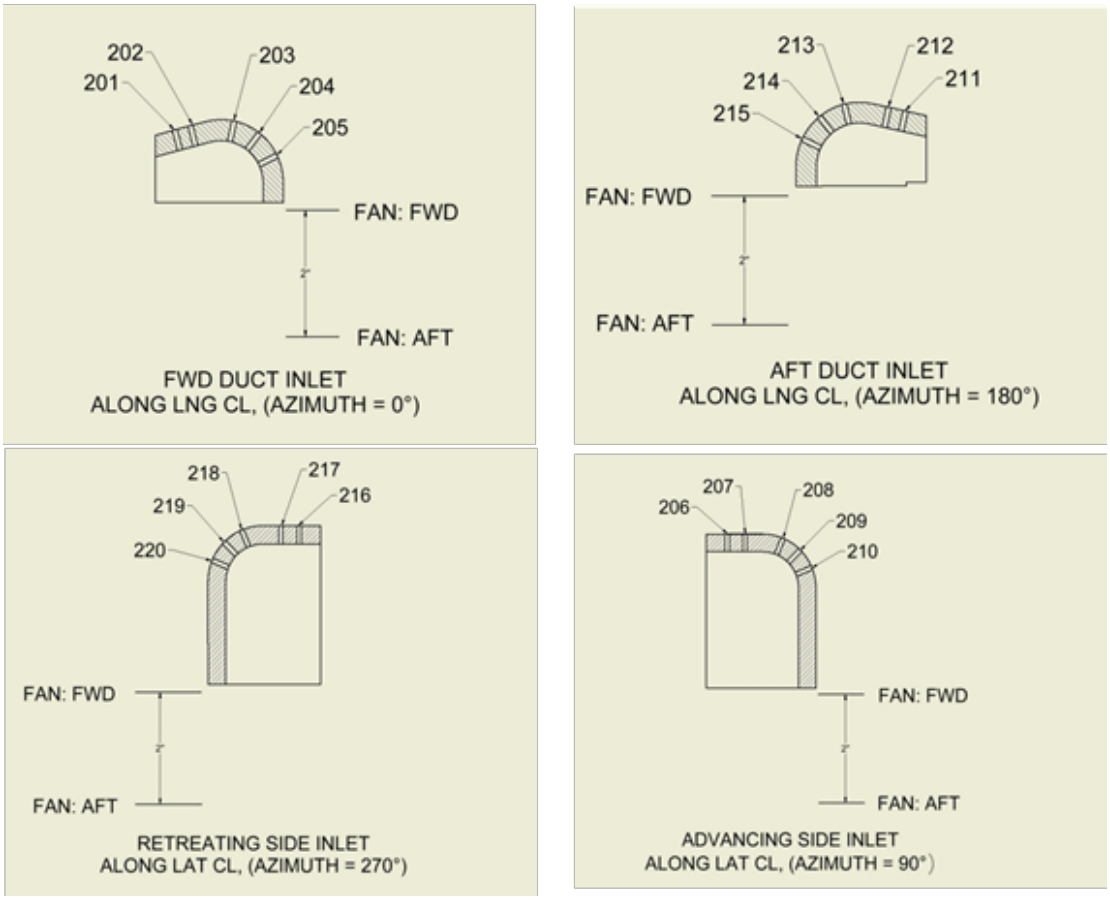

Figure 5: Schematic of pressures tap locations and indexes around duct inlet at azimuths = 0, 90, 180, 270 deg

repeated. Repeat data points were collected throughout testing to verify and validate the quality of the data. Dynamic tares with the blades removed were also gathered and will be used to correct the raw measurements. In addition, in order to improve the data set fidelity for predictive method validation, the effects of fan rotational direction as well as hub and drive-training fairings were acquired.

RESULTS AND DISCUSSION

The focus of this section is on the analysis of interactional aerodynamics, which consists of mainly the initial analysis of pressures measured near and around the duct inlet and fan aerodynamic performance with and without the surrounding wing. Pressure at each port was measured by a dedicated miniature pressure transducer connected directly to it. It should be noted that some of the test parameters in figures are deliberately not shown as this work is part of a larger double blind study with the concurrent development of an analytical model.

Pressures Near and Around Duct Inlet

The knowledge of the pressures at critical locations over the wing surfaces and particularly around the duct inlet is very important for understanding the mutual aerodynamic interactions between the fan and wing. While it is common that the duct or the shroud around the fan can, in general, contribute significant thrust and improve the hover efficiency for a generic lift fan, the degree and characteristics of the mutual aerodynamic interactions between the fan and the duct can differ significantly among different types of lift fans and in different flight regimes. Unlike the generic ducted fan that usually has a symmetric duct inlet along the circumference and relatively large duct depth, the duct inlet and nearby shape as well as the depth of the duct in a FIW configuration are severely constrained by the actual wing aerodynamic shape required for fast forward flight. Therefore, it is necessary to measure the pressures not only around one representative duct inlet section but also at multiple locations around the duct circumference in order to fully understand the wing pressure characteristics. As indicated in the model description section, pressure ports are located at sections every 30^o of azimuth around the duct circumference for the FIW model tested.

Figure 6 illustrates sample vector plots of pressures measured near and around the duct inlet at azimuth = 0^o and 180^o for three different fan collective pitch angles (2^o, 18^o and 38^o). The discrete dots in this figure represent contour points of the wing airfoil shape. The corresponding pressure tap indexes are from p201 to p205 for the leading edge section (azimuth = 0^o) and from p211 to p215 for the trailing edge section (azimuth = 180^o). The arrows represent the pressure directions (always normal to the local surface) and the magnitudes. Pressure is negative (suction) if the arrow points away from the surface, otherwise, it is positive. The following phenomena can be observed qualitatively from Fig. 6: first, at collective pitch angle = 2^o, all pressures are benign, which is an

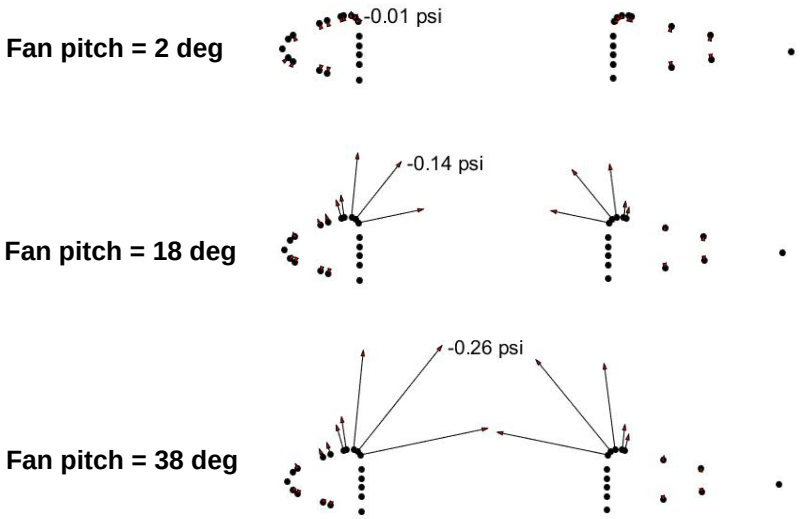

Figure 6: Vector plot of pressures around duct inlet

expected result (i.e., if there is little to no fan thrust then there should be no wing thrust in hover); second, suction (negative pressure) increases as the fan collective pitch increases, which indicates that the fan operating condition is a dominant factor affecting the wing pressures; and third, the magnitude of pressures on the leading edge section and trailing edge section appear asymmetric.

To quantitatively study the pressure characteristics near and around the duct inlet, only the magnitudes of pressure are presented in the following discussions. Figure 7 shows the corresponding values of pressure magnitude near and around the duct inlet (p201 - p205, as shown by the x-axis), for a blade loading coefficient of 0.153. Again, pressure taps p201 and p202 on the upper flat wing surface are called *near* the duct inlet pressures and other three pressure taps (p203–p205) are called *around* the duct inlet pressures. Figure 7 shows that for the blade loading coefficient of 0.153, all five pressures are negative, providing contributions to the positive wing or overall thrust. The effect of different fan thrust levels on duct pressures will be discussed later. Figure 7 also shows that while the largest suctions are generated around the duct inlet, the suctions on the flat wing surface near the duct inlet lip are significant too (approximately 25% of the ones around the duct inlet), which implies that the geometry or shape of the wing surface adjacent to the duct inlet should be integrated with the duct inlet design to generates as much thrust as possible for a FIW configuration.

To illustrate the effect of different fan collective pitches and thrust levels on the duct thrust, Figure 8 presents five reference pressures measured at the locations shown in Fig. 7 over a wide range of fan collective pitches. Notice that the pressure becomes more negative (i.e., more positive wing thrust is being generated) as the fan collective pitch increases and then stalls at a fan collective pitch of around 32^{o}. All five pressures show similar stall characteristics. Also, as concluded from analyzing Fig. 7, for all fan collective pitches, while the pressures around the duct inlet (p203 to p205) constitute large contributions to the wing thrust, the pressures near the duct inlet (p201 and p202) make sizeable contributions too. To further understand the relationship between the duct pressure and the fan thrust characteristics, the fan blade loading coefficients measured by the independent fan balance are also plotted in Fig. 8, as represented by the right y-axis. The results indicate that the fan thrust has a very similar trend to the pressures near and around the duct inlet, which is expected, but stalls at a fan collective pitch of approximately 4^{o} higher than the duct pressures, which implies that a higher overall maximum FIW thrust could be achieved if the duct inlet and the wing surface could be optimized to delay the

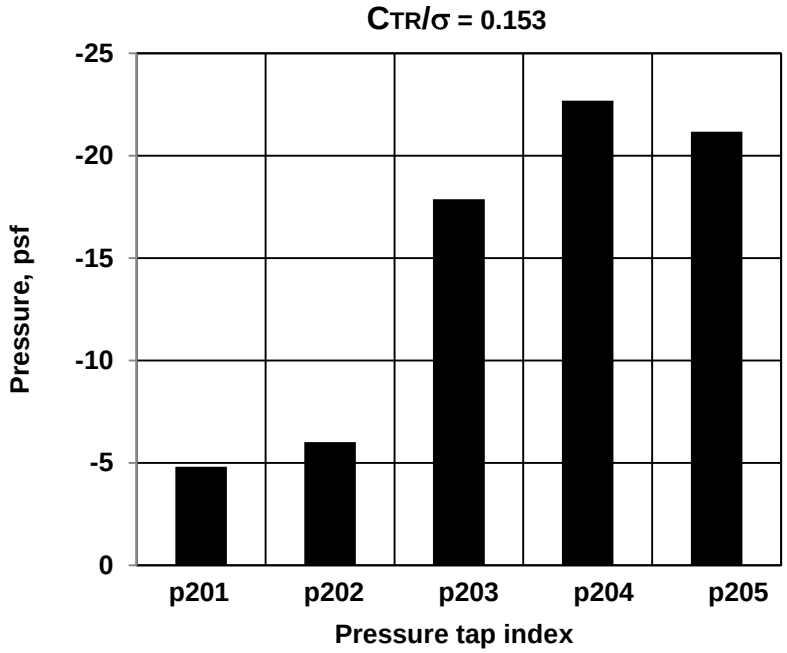

Figure 7: Pressure measured around duct inlet at azimuth = 0 deg.

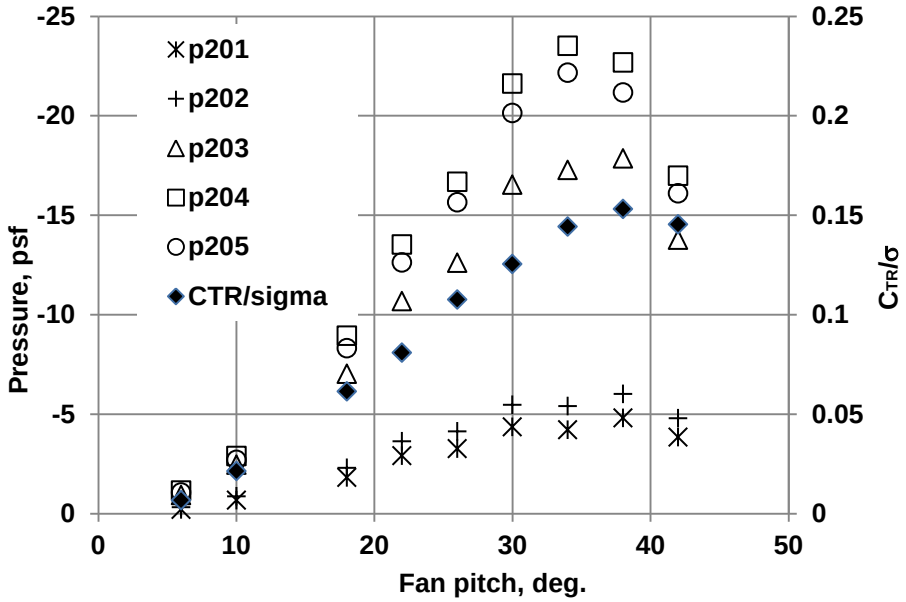

Figure 8: Effect of fan operating condition on duct pressures at azimuth = 0 deg.

duct pressure stall and therefore to improve the maximum pressures on the wing.

For a symmetrical ducted fan, the pressure at a given relative inlet location around the duct does not change around the duct circumference in hover because the curvature of the duct inlet and the fan position within the duct remain unchanged. However, for the FIW configuration, the wing chordwise thickness changes continuously, and consequently, the wing surface curvature/shape near the duct inlet can be different along the duct circumference in order to make the transition from the wing surface to the duct inlet aerodynamically smooth. Also, relative to the duct inlet, the fan axial location within the duct can be different at different wing chordwise locations. Thus, to understand the aerodynamic interactions between the fan and wing, it is necessary to understand if and how the duct pressure changes around the duct circumference. Figure 9 presents the pressures at the duct inlet lip (the middle pressure tap around the duct inlet) for every 30^o azimuth angle for a given fan operating condition. It is clearly shown that the pressures at the inlet lip vary significantly along duct circumference with the maximum suction at the zero azimuth angle (leading edge) and the minimum suctions at both advancing (90^o) and retreating (270^o) sides. It is noticed that the duct inlet radius is 1 inch and remains constant along the duct circumference for this FIW model. This large pressure variation along the duct circumference can be caused by either the wing surface shape near the duct inlet or the fan position within the duct, which implies that there is potential to further improve the wing contributions to the overall thrust by improving the transition from the wing surface to the duct inlet around the duct circumference and the fan axial position within the duct.

To further investigate the effects of fan operating conditions on pressures along the duct circumference, Figure 10 shows the pressures at the duct inlet lip at four representative circumference locations (azimuth angles = 0^o, 90^o, 180^o and 270^o). This figure shows that the overall trend of each pressure at different fan collective pitches is similar to each other with the high values observed at the duct leading edge and the low values at the advancing and retreating sides. All four pressures show stall at almost the same fan collective pitch (approximately 34 deg.), which indicates that the fan operating condition might be the only dominating factor that affect the wing pressure stall.

To identify the effect of fan axial position within the duct on the wing and fan aerodynamic performance, two different fan positions were tested. Figure 11 compares the corresponding pressures measured around the forward duct inlet at zero azimuth position (p201 – p205). Pressures presented in this figure are rescaled by dividing the corresponding blade loading coefficient in order to identify the effect of fan position only. This figure indicates that all five pressures are very sensitive to the fan position with the aft fan position resulting in a larger suction around the duct inlet. This result clearly reveals that the fan position should be one of the design parameters in FIW design even through the duct depth is relatively shallow compared to conventional ducted fans.

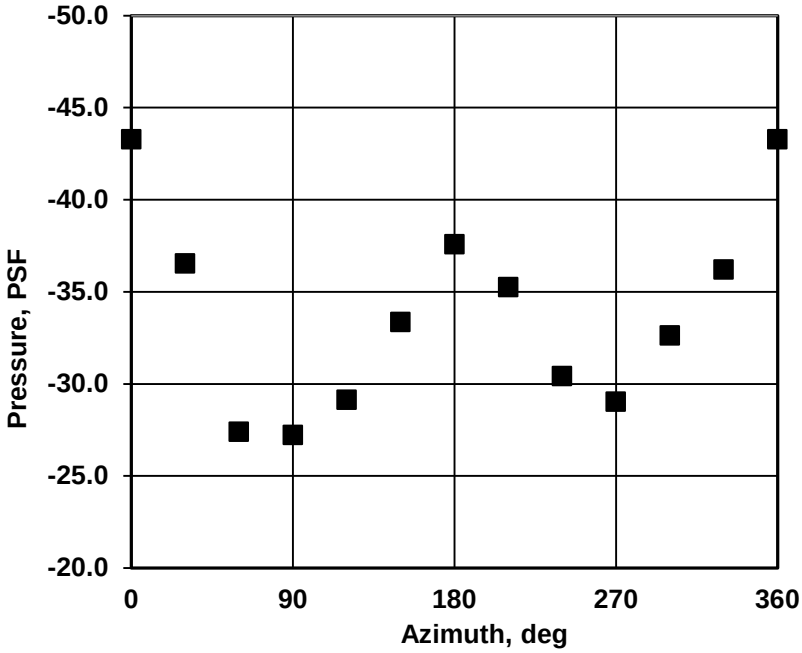

Figure 9: Variation of pressure at duct inlet lip around duct circumference

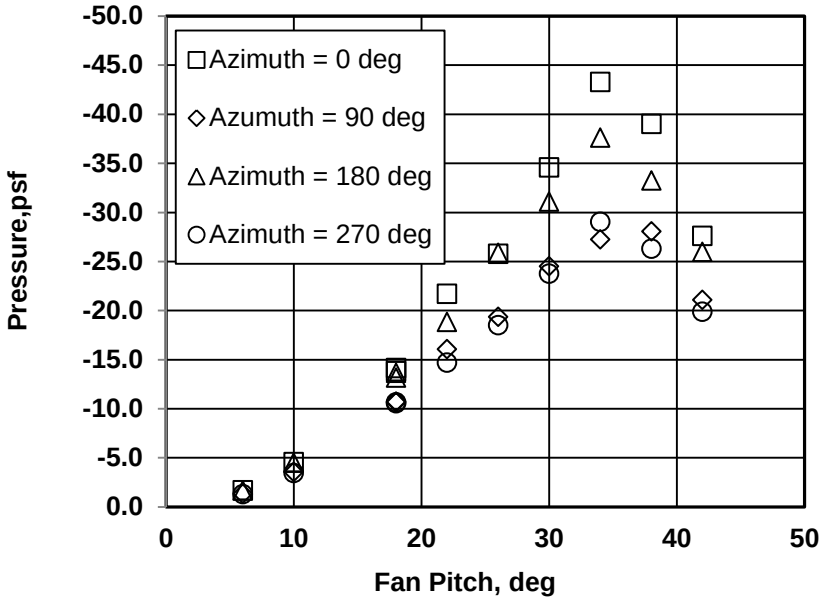

Figure 10: Effects of fan collective pitch on pressures at duct inlet lip

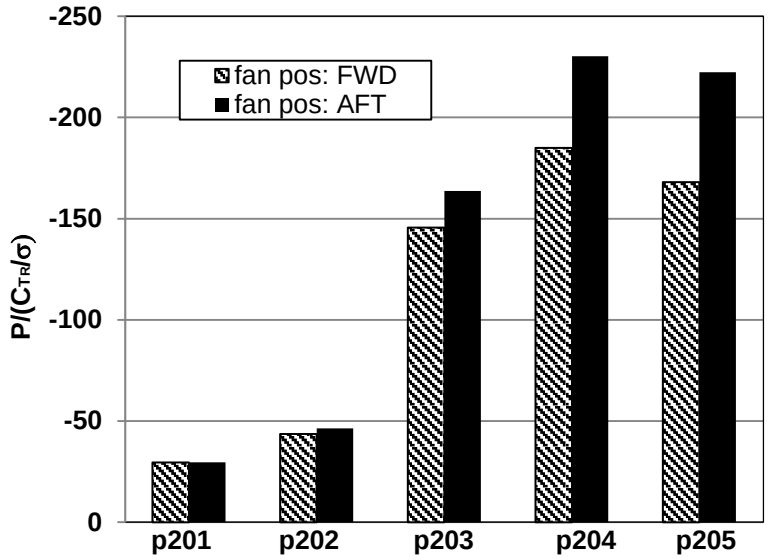

Figure 11: Effects of fan position within duct on duct pressure at azimuth = 0

Fan Performance with and without Wing

To fully exploit the benefits of the FIW configuration, in addition to having a good understanding of the wing thrust induced by the fan, the changes in the fan performance due to the existence of the wing must also be understood. Tests were conducted in two steps: the isolated fan only and the complete FIW configuration. Figure 12 shows the corresponding aerodynamic performances for the isolated fan and the fan with the surrounding wing. Apparently, they are very different. One of the obvious changes in the fan performance is that before a fan pitch angle of 30^{o} (approximately where the isolated fan stalls), the isolated fan generates a much higher fan blade loading. In other words, the fan itself generates much less thrust for a given collective pitch when having the surrounding wing. This implies that the induced velocities or the induced angle of attack at the fan disk are larger when the fan is in the FIW than the isolated fan at a constant fan collective pitch. This large difference in the induced angle of attack or in the effective angle of attack should be considered when designing a fan system for the FIW configuration.

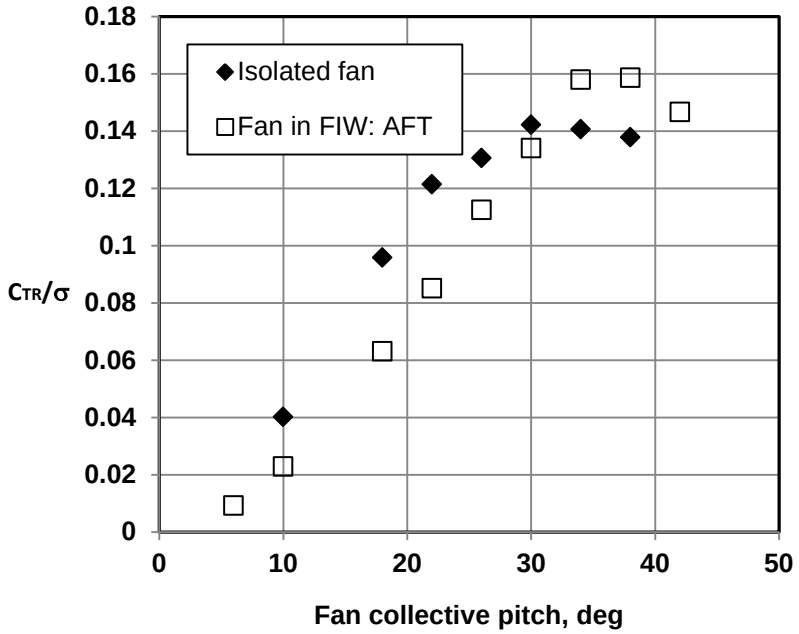

Figure 12: Fan aerodynamic performance with and without wing

Another difference in fan aerodynamic characteristics is the maximum thrust the fan can generate with and without the surrounding wing. The fan maximum thrust capability in hover is critical to the FIW configuration because the size of the fan is always constrained by the space available in the wing. Figure 12 shows that the maximum fan thrust is increased by more than 10% when operating in the wing, which is very significant because this result demonstrates that in addition to the beneficial aerodynamic effects of the fan on the wing, the wing enhance the maximum fan thrust too. These mutually beneficial aerodynamic effects between the fan and wing should be fully understood and exploited in the FIW configuration design.

Based on simple two-dimensional momentum theory for a generic ducted fan, the efficiency can be improved by approximately 30% and the maximum thrust can be doubled relative to the same size isolated or un-ducted fan in hover. To understand the overall performance improvement for the FIW configuration over the isolated fan in hover, Fig. 13 shows the thrust vs the power required for both the isolated fan and the FIW. The effects of fan position within the duct have also been shown in this figure. Clearly, the FIW has a much larger thrust capability due to both the wing contribution to the overall thrust and the improvement in maximum fan thrust just discussed. Further analysis shows that for the current FIW model, the wing thrust is approximately 50% of the fan thrust in hover. Also, it is clear that the FIW is more efficient than the isolated fan and that approximately an 8% higher maximum thrust is generated when the fan is positioned at the aft position within the duct.

SUMMARY AND CONCLUSIONS

A series of wind tunnel tests were successfully conducted to study the aerodynamic performance of an isolated fan and a fan-in-wing configuration as well as the aerodynamic interactions between the fan and wing in hover. An independent fan balance and an innovative motion limiting mechanism were specifically developed for this test. A parametric study of key fan design parameters was systematically conducted, which included fan rpm, blade collective pitch and twist distribution, number of fan blades, fan solidity, and fan axial location within the duct. A large volume of data with more than 3000 test conditions was obtained, from which a benchmark data set is being established to support the validation of CFD and other predictive models and to provide a better understanding of fan and wing aerodynamic interactions.

For the isolated fan test, both a tunnel balance and a fan balance were used simultaneously to measure the fan thrust to ensure the accuracy of the fan balance measurement. For the complete FIW configuration test, the tunnel balance was used to measure all six components of force and moment for the complete FIW model while the fan balance was used to independently measure the fan thrust only. In addition to the force data, 169 pressure taps were distributed over the upper and lower wing surfaces, near and around the duct inlet, and over the walls inside the duct. This paper focused on the initial analysis of the interactional aerodynamics between the fan and wing including the representative pressures near and around the duct inlet, and the fan performance with

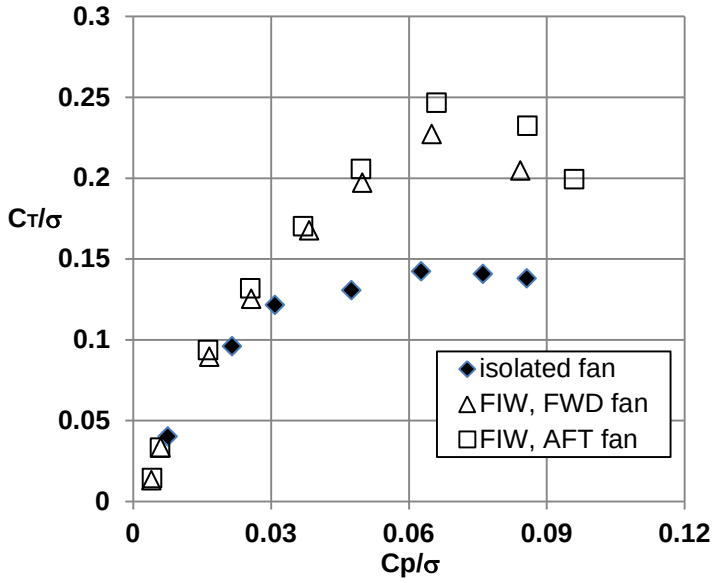

Figure 13: Aerodynamic performance comparison between isolated fan and FIW

and without the surrounding wing. While more comprehensive and systematic analysis is being conducted, the initial analysis shows clearly that the aerodynamic interactions between the fan and wing are mutually beneficial, which provides strong evidences that an integrated design philosophy for the fan and the wing should be adapted to optimize the overall aerodynamic performance of FIW configurations. The following are some observations and conclusions drawn from the initial study:

1. The aerodynamic interaction between the fan and the wing were strong and mutual in hover. Results showed that the fan aerodynamic characteristics were altered significantly when the fan was embedded within the wing. The changes included that the fan experienced a much larger induced angle of attack and stalled at a higher fan collective pitch. In addition, test results revealed that the maximum fan thrust was increased by more than 10% with the surrounding wing. These results are very useful for the future fan development and provide direct evidence that the fan and the wing should be considered as one integrated system in the FIW configuration design.

2. In addition to the pressures directly around the duct inlet, the pressures on the wing skin near the duct inlet were also significant. Their vales were as large as approximately 25% of the ones directly around the duct inlet. It should be noticed that relative to a conventional ducted fan, there is a lot of surface available near the duct for the FIW configuration. Therefore, if more of the wing surface that is not very close to the duct can be used to generate the thrust through optimizing the design between the wing and the duct inlet or by using flow control technique, the FIW hover efficiency can be further enhanced.

3. For the fan-in-wing configuration, unlike a symmetrical ducted fan, the pressures (suctions) near and around the duct inlet varied significantly around the duct circumference. The pressures at both sides (azimuth = 90^o and 270^o) were only approximately 60 - 75% of the ones around the forward and aft sections (azimuth = 90^o and 270^o). To further improve the pressures on the surfaces near both sides of the duct needs to be exploited to enhance the FIW aerodynamic performance.

4. The wing made significant contributions to the overall thrust and its thrust was approximately 50% of the fan thrust in hover. As expected, the wing thrust/pressure depends on the fan operation conditions. However, the wing pressures and fan thrust had different stall characteristics. The wing pressures stalled at a lower (approximately 4^o fan pitch lower) than the fan thrust.

5. The fan and overall FIW performance was sensitive to the fan position within the duct. Approximately 9% more thrust was generated when the fan was placed at the aft fan position within the duct.

ACKNOWLEDGMENTS

The authors would like to thank the Office of Naval Research for their support with Mr. John Kinzer as the technical monitor. The authors would also like to thank Mr. Fred Behnaz for his creative and diligent efforts in model design and fabrication.

REFERENCES

1. http://www.darpa.mil/Our_Work/TTO/Programs/Vertical_Takeoff_and_Landing_Experimental_Plane_(VTOL_X-Plane).aspx
2. http://boeing.mediaroom.com/Boeing-Phantom-Swift-Selected-for-DARPA-X-Plane-Competition
3. http://www.defensenews.com/story/defense/air-space/2016/03/04/darpas-vertical-takeoff-x-plane-contract-goes-aurora/81309356/
4. https://en.wikipedia.org/wiki/Ryan_XV-5_Vertifan
5. http://www.hightech-edge.com/northrop-grumman-muvr-fan-in-wing-high-speed-vtol-aircraft/12203/
6. http://defense-update.com/products/v/various_ucav.htm
7. https://en.wikipedia.org/wiki/Urban_Aeronautics_X-Hawk
8. N. P. Bi, A. J. Sydney, K. R. Kimmel, D. J. Haas, “Experimental Investigation of Fan Aerodynamic Performance for Fan-In-Wing Applications”, Presented at the American Helicopter Society 71st Annual Forum, May 3 – 5 2015, Virgina Beach, VA.
9. A. J. Sydney, N. P. Bi, K. R. Kimmel, D. J. Haas, “Experimental Investigation of Fan-In-Wing Aerodynamic Performance In Hover”, Presented at the American Helicopter Society 72nd Annual Forum, May 17 – 19 2016, West Palm Beach, FL.